THE TURBULENT STATISTICS IN THE WAKE OF A SHORT STACK

Muyiwa S. Adaramola
Division of Environmental Engineering
University of Saskatchewan
57 Campus Drive, Saskatoon, Saskatchewan, Canada S7N 5A9
muyiwa.adaramola@usask.ca

Donald J. Bergstrom
Department of Mechanical Engineering
University of Saskatchewan
57 Campus Drive, Saskatoon, Saskatchewan, Canada S7N 5A9
don.bergstrom@usask.ca

David Sumner
Department of Mechanical Engineering
University of Saskatchewan
57 Campus Drive, Saskatoon, Saskatchewan, Canada S7N 5A9
david.sumner@usask.ca

ABSTRACT

The characteristics of the turbulent statistics along the wake centreline of a stack was experimentally studied in a low-speed wind tunnel using thermal anemometry. The cross-flow Reynolds number was $Re_D = 2.3\times10^4$, and the jet-to-cross-flow velocity ratio was varied from $R = 0$ to 3. The stack was partially immersed in a flat-plate turbulent boundary layer, with a boundary layer thickness-to-stack-height ratio of $\delta/H = 0.5$ at the location of the stack. The turbulent statistics are found to be strongly influenced by the value of R. The Reynolds shear stress and the triple correlation were strongly influenced by the local velocity gradient, especially for lower values of R within the stack wake and within the jet wake for higher values of R within the jet wake. The skewness and flatness factors indicated a strong deviation from a Gaussian distribution, which is evidence of the complexity of the flow.

INTRODUCTION

This study consider the complex flow field associated with a stack. A uniform finite circular cylinder represents a stack with no jet flow issuing from the stack. The separated shear flow from the sides of the cylinder interacts with the downwash flow from the free end and with the upwash flow from the ground plane. These interactions make the flow field behind the finite cylinder complex and strongly three-dimensional. There are marked changes in the near-wake flow structure along the cylinder height, and these changes are strongly influenced by the cylinder's aspect ratio, AR (= H/D, where H and D are the height and diameter of the cylinder, respectively). The turbulent wake of the finite cylinder is characterized by a counter-rotating pair of tip vortices originating near the free end, which induces a strong downwash velocity along the wake centreline and interacts in a complex manner with Kármán vortex shedding. For cylinders of small AR, the flow around the free end may suppress Kármán vortex shedding, and a distinct wake structure is observed (Sumner *et al*., 2004; and Tanaka and Murata, 1999). The critical AR below which Kármán vortex shedding is suppressed is a function of AR and δ/H (where δ is the boundary layer thickness on the ground plane). When the AR exceeds this critical value, another pair of streamwise vortex structures, known as the base vortex structures, is found within the flat-plate boundary layer on the ground plane closer to the base of the cylinder. For a cylinder of AR = 9, Adaramola *et al*. (2006) observed a region of high turbulence intensity behind the cylinder, which was centred between the tip and base vortex structures.

The presence of a jet flow issuing from the stack gives rise to an even more complicated flow structure, both around the stack and in its wake. The flow field is characterized by the complex interactions between the jet and stack wakes, shear produced by the upward momentum of the jet, and downwash flow (Huang and Hsieh, 2002 and 2003). For a non-buoyant jet, the extent of this complexity depends on the jet-to-cross-flow velocity ratio, R (= U_e/U_∞, where U_e is the jet exit velocity and U_∞ is the freestream velocity). The flow regimes in the stack wake have been classified differently by different authors. Huang and Hsieh (2002, 2003), for example, classified the stack and jet wake flow patterns into four regimes based on the approximate value of R: (i) downwash flow ($R < 0.95$), (ii) cross-wind-dominated flow ($0.95 < R < 1.4$), (iii) transitional flow ($1.4 < R < 2.4$), and (iv) jet-dominated flow ($R > 2.4$). The classification was made based on their studies of the flow topology in the vertical plane along the wake centreline for a stack of AR = 25 and $d/D = 0.78$ operating at $Re_D = 2074$ (based on stack

diameter, D) and Re_d = 200 to 8×10^3 (based on jet exit diameter, d). Adaramola *et al*. (2007), on the other hand, identified three distinct flow regimes when the value of R was varied between 0 and 3. The flow regimes are the downwash flow ($R < 0.7$), the cross-wind-dominated flow ($0.7 \leq R < 1.5$), and the jet-dominated flow ($R \geq 1.5$) regimes. Each flow regime had a distinct structure to the mean velocity and turbulence intensity fields. They also reported that there is a strong influence of R on the variation of the Strouhal number, St ($= f_s D/U_\infty$, where f_s is the vortex shedding frequency and U_∞ = freestream velocity), along the stack height. In addition, for $R \geq 1.5$, they observed a two-cell structure behaviour in St along the height of the stack. In agreement with Eiff *et al.* (1995) and Eiff and Keffer (1999), the value of St within the stack and jet wakes was the same (for a particular value of R), which suggested that vortices with the same frequency are being shed in both wakes.

Given the complex wake structure of this flow, and its significant variation with R, it is of interest to document the turbulence field, both in terms of second-and third-order moments. Using a boundary layer X-probe, streamwise and wall-normal velocity components were measured in a vertical plane along the centreline and downstream of the stack. This paper presents a preliminary analysis of the turbulence statistics in the stack and jet wake based on these two fluctuating velocity components.

EXPERIMENTAL APPROACH

The present experiments were conducted in a low-speed, closed-return wind tunnel with a test section of 0.91 m (height) × 1.13 m (width) × 1.96 m (length). The streamwise freestream turbulence intensity was less than 0.6% and the velocity non-uniformity outside the test section wall boundary layers was less than 0.5%. The test section floor was fitted with a ground plane. A roughness strip located about 200 mm from the leading edge of the ground plane was used to enhance the development of a turbulent boundary layer. At the location of the stack (with the stack removed), the boundary layer provided a thickness-to-height ratio of $\delta/H \approx 0.5$, and the Reynolds number based on momentum thickness, θ, was $Re_\theta = 8\times10^3$. The experimental set-up for the study is shown schematically in Fig. 1, and was similar to that adopted by Adaramola *et al*. (2007).

Experimental Apparatus

A cylindrical stack of H = 171.5 mm, D = 19.1 mm, d/D = 0.67, and AR = 9, was used in the present study. The stack was located 700 mm downstream of the roughness strip on the ground plane. The experiments were conducted at a single stack Reynolds number (based on D and U_∞) of $Re_D = 2.3\times10^4$. The exhaust velocity of the non-buoyant stack jet was varied with two MKS 1559A-200L mass flow controllers arranged in parallel. The jet-to-cross-flow velocity ratio was varied from R = 0 (no jet exiting the stack) to R = 3, corresponding to momentum flux ratios of R_m (R^2) = 0 to 9. The jet Reynolds number, Re_d (based on d and U_e) ranged from 7.6×10^3 to 4.7×10^4.

Measurement Instrumentation

The wind tunnel data were acquired by a computer with a 1.8-GHz Intel Pentium 4 processor, a National Instruments PCI-6031E 16-bit data acquisition board, and LabVIEW software. The freestream conditions were obtained with a Pitot-static probe (United Sensor, 3.2-mm diameter), Datametrics Barocell absolute and differential pressure transducers, and an Analog Devices AD590 integrated circuit temperature transducer.

Profile measurements were made with a TSI model 1243-20 boundary layer X-probe and a constant-temperature TSI IFA-100 anemometer. The X-probe was oriented to measure the streamwise, u, and wall-normal, w, velocity components. The probe was manoeuvred to the measuring points using the wind tunnel's three-axis computer-controlled traversing system. At each measurement point, 100,000 instantaneous velocity data per channel were acquired at a sampling rate of 10 kHz per channel after low-pass filtering at 5 kHz. The uncertainties in the streamwise and wall-normal fluctuating velocity components were estimated to be ±4% and ±7%, respectively, while the uncertainty in the Reynolds shear stress was estimated to be ± 9%. For a given value of the velocity ratio, R, the profile measurements were made along the centre plane of the stack wake and jet wake at x/D = 10, 15 and 20. The measurement plane extended to z/D = 14 in the wall-normal direction.

RESULTS AND DISCUSSIONS

In this paper, measurements for three values of R = 0.5 (downwash flow regime), R = 1 (cross-wind-dominated flow regime) and R = 2.5 (jet-dominated flow regime), which represent the three distinct flow regimes identified by Adaramola *et al.* (2007), are presented and discussed. In addition, the data for R = 0, which represent the finite circular cylinder case, are also included. Due to space constraints, only the results at a streamwise distance of x/D = 10 are presented in this paper. Following the definition of Eiff and Keffer (1999), the stack wake is defined as the region $0 < z/H \leq 1$, while the region of $z/H > 1$ is the jet wake.

Time-averaged velocity profiles

The time-averaged streamwise velocity profiles for R = 0, 0.5, 1 and 2.5 at x/D = 10 along the wake centre plane are presented in Figure 2. For R = 0, corresponding to no jet flow, a strong velocity defect occurs within the stack wake and the minimum value of the mean velocity profile is located within the boundary layer (δ/H = 0.5) on the ground plane. The vertical location of the minimum value of the mean velocity decreases, and the minimum values increases, as the streamwise distance from the stack increases (not shown). A similar profile is observed when R = 0.5, which

represents the downwash flow regime, but with the presence of another, but smaller, velocity defect region near the free end of the stack, indicating the presence of the jet that obstructs the cross-flow (Onbaşioğlu, 2001).

In the case of the cross-wind-dominated flow regime, R = 1, the mean velocity profile is different from those for R = 0 and 0.5. The main velocity defect in the stack wake is reduced, while within the jet wake, the second region of velocity defect increases in size and magnitude and is shifted upwards towards the free end of the stack compared with R = 0.5. This stack wake merges with a second wake region, called the jet wake, above the stack free end.

For the jet-dominated flow regime, when R = 2.5, the largest velocity defect still occurs within the stack wake, with the minimum value of the mean velocity profile located above the ground plane boundary layer. The second velocity defect region is now well above the stack free end, better defined and more isolated from the stack wake. In addition to these wake features, there is another region in these profiles that corresponds to the jet flow where $u/U_\infty > 1$, which is associated with the jet rise. The peak of this region corresponds to the centre of the jet flow. The jet centreline at x/D = 10 is located at z/H = 1.41 above the ground plane.

The time-averaged wall-normal velocity profiles at x/D = 10 along the centre plane are shown in Figure 3. These profiles show two distinct flow regions within the stack and jet wakes: the upwash flow region which occurs closer to the base of the stack, and the downwash flow region which occurs in the upper half of the stack wake. The profiles for R = 0, 0.5 and 1 are all similar but differ in the relative location of the downwash flow region which moves upward toward the free end of the stack as R increases. The absolute magnitude of the downwash flow also reduces with R. For R = 2.5, the downwash flow region is smaller. Another upwash flow, which is a direct consequence of the jet flow, is also observed above the stack free end and within the jet wake.

Streamwise turbulent intensity

The streamwise turbulent intensity (u'/U_∞) profiles are shown in Figure 4 for different values of R. This information is equivalent to the streamwise normal Reynolds stress. For each value of R, the turbulent intensity varies along the stack height and approaches zero above the stack free end for R = 0, and above the jet flow region for R = 0.5, 1 and 2.5. The wall-normal turbulence intensity (w'/U_∞) profiles (not shown) are similar to the streamwise turbulence intensity data for all values of R. For R = 0 and 0.5, there is a localized region of high streamwise turbulence intensity within the stack wake. This high turbulence intensity behind the stack is attributed to the interactions between the streamwise vortex structures, the downwash from the free end, and the upwash from the ground plane, which produces strong shear (Sumner *et al*., 2004). This region coincides with a region of large velocity deficit (see Figure 2) in the stack wake.

When R = 1, a second region of high streamwise turbulence intensity appears just above the free end of the stack and within the jet wake. The second region may be due to the separated shear flow from both sides of the jet flow and the interaction of the jet flow with the cross-flow. This second region coincides with a region of velocity deficit (see Figure 2) in the jet wake. For R = 2.5, the second region of high turbulence intensity within the jet wake is now well defined. The peak turbulence intensity values in the jet wake are smaller in magnitude compared to the highest turbulence values within the stack wake.

Reynolds shear stress and triple correlation

Due to the limitation of the instrument used, only the component of the Reynolds shear stress in the x-z plane was measured. Figure 5 presents measurements of the Reynolds shear stress, $-\langle uw\rangle/U_\infty^2\rangle$, which physically relates to the transport of momentum due to the turbulent fluctuations in the flow. Regions of elevated Reynolds shear stress may be associated with strong production of turbulence, which depends on the local velocity gradients. The behaviour of the Reynolds shear stress can be deduced from the mean velocity profile (see Figure 2), especially for lower values of R within the stack wake and for higher values of R within the jet wake. For R = 0 and 0.5, there are two regions of elevated Reynolds shear stress, each of opposite sign, located behind the stack, similar to what was reported by Adaramola *et al*. (2006) for a finite circular cylinder of AR = 9. The region of positive Reynolds shear stress is located in the region of downwash flow from the free end of the stack, while the negative Reynolds shear stress region occurs within the ground plane boundary layer in the region of upwash flow.

When R = 1, there is a reduction in the magnitude of the Reynolds shear stress within the upwash flow region compared with R = 0 and 0.5. In addition, another negative Reynolds shear stress region is observed close to the stack free end and a region of positive elevated Reynolds shear stress within the jet wake. This may be due to the mixing of the jet flow with the cross-flow that increases the turbulence within this region.

When R = 2.5, the Reynolds shear stress is entirely negative in the upper half of the stack wake, and two regions of elevated Reynolds shear stress, each of opposite sign, are observed in the jet wake. The negative Reynolds shear stress is located just above the stack free end and has a smaller absolute value than the strong positive Reynolds shear stress that occurs inside the jet wake. In addition, another smaller, positive shear stress region is observed below the mid-height of the stack.

The profiles of $\langle u^2w\rangle/ U_\infty^3$, which relate to the transport of $\langle u^2\rangle$ by the turbulent motion in the wall-normal direction, are shown in Figure 6, for different values of R. These profiles are similar to the Reynolds shear stress profiles except that they have lower magnitude. When R = 0 and 0.5, one negative and one positive peak are observed, each of which occur below and above the mid-span of the stack, respectively. When R = 1, a strong negative peak is observed within the boundary layer region and two positive

peaks, one below the stack free end and the other within the jet wake region, are seen.

When $R = 2.5$, the profile of $\langle u^2 w \rangle / U_\infty^3$ at $x/D = 10$ has alternately two negative and two positive peaks. The negative peaks are located within the ground plane boundary layer and near the free end of the stack, while a weak positive peak is located within the stack wake and a strong positive peak is located inside the jet wake.

Skewness and flatness factors

The skewness and flatness factors can be used to provide information about the distribution of the velocity fluctuation around its mean value. A non-zero value of the skewness factor indicates the degree of temporal irregularity in the fluctuation and a flatness factor more than 3 is attributed to a "peaky signal" (Gad-el-Hak and Bandyopadhyay, 1994), due to irregular turbulent events.

The skewness profiles for the streamwise velocity component ($S_u = \langle u^3 \rangle / (u')^3$) are presented in Figure 7 for different values of R. The existence of an asymmetry in the fluctuation is shown by the non-zero value of the skewness factor for all values of R. In general, two regions of elevated peak values, each of opposite sign, are observed within the combined stack and jet wakes. The positive region is observed to occur immediately above the negative region. However, the specific locations and absolute values of these peaks depend on R. The negative region indicates the occurrence of the arrival of low-speed fluid from the ground plane and the stack wake as a result of the upwash flow motion. The positive region indicates the occurrence of the arrival of high-speed fluid due to the downwash flow from the outer region above the combined stack and jet wake.

For $R = 0$, these two regions are located just below the stack free end. The skewness factor is almost independent of the downstream distance (not shown), especially within the base region and above the free end of the stack. For $R = 0.5$, the negative peak region occurs at the stack free end while the positive peak region has almost disappeared. In addition, the numerical value of the negative peak region of S_u is higher for $R = 0.5$ than $R = 0$. This may be due to the presence of a weak jet flow, which increases the amount of low-speed fluid in this region and the mixing of the jet fluid with the cross-flow fluid. The almost non-existence of the positive peak region may be due to the strong effect of the cross-flow on the jet flow.

In the case of $R = 1$, the two peak regions are completely above the stack free end. Compared with $R = 0$ and 0.5, the absolute value of the positive peak is much higher. This is due to the interaction between the cross-flow and the jet flow. For $R = 2.5$, within the stack wake, the skewness factor is only slightly less than the corresponding Gaussian probability distribution of zero. Relatively weak negative and strong positive regions are observed within the jet wake and occur at a relatively higher position above the ground plane, when compared with lower values of R. The skewness factor behaviour within the jet wake shows the strong interaction between the cross-flow and the jet flow.

The streamwise flatness factor ($F_u = \langle u^4 \rangle / (u')^4$) profiles are shown in Figure 8. For all values of R, a region with a flatness factor larger than 3 is observed. The largest values (> 3) of the flatness factor occur in a region mid-way between the negative and positive regions of the streamwise skewness factor (see Figure 7). The behaviour of F_u indicates that there are strong intermittent turbulent events within the stack and jet wake.

For $R = 0$, the large value of F_u which occurs near the stack free end may be the result of the tip vortex structures (see e.g., Sumner *et al.*, 2004) and the downwash flow from the stack free end that gives rise to the observed strong intermittent behaviour. A similar behaviour is noted for $R = 0.5$, except that the numerical values of F_u are smaller (less intermittency) near the stack free end compared with $R = 0$. This indicates that the weak jet and downwash flow from the stack free end tends to stabilize the flow. In the case of $R = 1$ and 2.5, this intermittency now occurs in the jet wake and is associated with jet flow structures and mixing between the cross-flow and jet flow. The relative location of this region above the ground plane increases with R.

CONCLUSIONS

In this study, the effect of the jet-to-cross-flow velocity ratio, R, on the behaviour of the turbulent statistics within the wake of a short stack is investigated experimentally using two-component thermal anemometry. In the downwash flow regime ($R = 0.5$), two elevated regions, one negative region within the ground plane boundary layer and another positive region just above the mid-height of the stack, are observed in the Reynolds shear stress profiles. The negative region may be due to the upwash flow from the ground plane, while the positive region coincides with the downwash flow region within the stack wake. For the cross-wind-dominated flow regime ($R = 1$), two negative peaks and one positive peak are observed within the stack wake, and another positive region above the stack free end. The positive region above the stack free end is due to the presence of the jet flow. The positive region in the Reynolds shear stress profile within the jet wake becomes stronger for the jet-dominated flow ($R = 2.5$) compared to the cross-wind dominated flow due to the stronger interaction between the jet flow and cross-flow. The velocity ratio R is also found to have a strong effect on the $\langle u^2 w \rangle U_\infty^3$ profile within the stack and jet wake.

The streamwise skewness and flatness factor profiles show a deviation from the Gaussian distribution of 0 and 3, respectively, especially toward the stack free end for $R < 1$; above the stack free end for $R = 1$; and within the jet wake for $R = 2.5$. In the case of $R < 1$, this deviation may be due to the interaction between the tip vortex structures and the downwash flow that gives rise to strong turbulent events. For $R \geq 1$, this deviation may be a result of the jet wake vortex and the strong the interaction between the jet flow and the cross-flow within the jet wake.

Based on the limited results presented in this paper, this study has demonstrated the complexity of the flow structure within the combined wake of a stack and jet flow. It appears

that the jet can affect the stack wake in a complex manner. Further study of this flow should also include measurements in the spanwise and wall-normal plane.

REFERENCES

Adaramola, M.S., Akinlade, O.G., Sumner, D., Bergstrom, D.J., Schenstead A.J., 2006. Turbulent wake of a finite circular cylinder of small aspect ratio. *Journal of Fluids and Structures*, 22, 919-928

Adaramola, M.S., Sumner, D., Bergstrom, D.J., 2007. Turbulent wake and vortex shedding for a stack in a cross-flow. *Journal of Fluids and Structures*, accepted.

Eiff, O.S., Kawall, J.G., Keffer, J.F., 1995. Lock-in of vortices in the wake of an elevated round turbulent jet in a crossflow. *Experiments in Fluids,* 19, 203-213.

Eiff, O.S., Keffer, J.F., 1997. On the structures in the near wake region of an elevated turbulent jet in a crossflow. *Journal of Fluid Mechanics*, 333, 161-195.

Eiff, O.S., Keffer, J.F., 1999. Parametric investigation of the wake-vortex lock-in for the turbulent jet discharging from a stack. *Experimental Thermal and Fluid Science,* 19, 57-66.

Gad-el-Hak, M., Bandyopadhyay, P.R., 1994. Reynolds number effects in wall-bounded turbulent flows. *Applied Mechanics Review*, 47, 307-365.

Hsieh, R.H., Huang, R.F., 2003. Tomographic flow structures of a round jet in a crossflow. *Journal of the Chinese Institute of Engineers,* 26, 71-80.

Huang, R.F., Hsieh, R.H., 2002. An experimental study of elevated round jets deflected in a crossflow. *Experimental Thermal and Fluid Science,* 27, 77-86.

Huang, R.F., Hsieh, R.H., 2003. Sectional flow structures in near wake of elevated jet in a crossflow. *AIAA Journal,* 41, 1490-1499.

Onbaşıoğlu, S.U., 2001. On the simulation of the plume from stacks of buildings. *Building and Environment* 36, 543-559.

Sumner, D., Heseltine, J.L., Dansereau, O.J.P. 2004. Wake structure of a finite circular cylinder of small aspect ratio. *Experiments in Fluids*, 37, 720-730.

Tanaka, S., Murata, S., 1999. An investigation of the wake structure and aerodynamic characteristics of a finite circular cylinder. *JSME International Journal, Series B: Fluids and Thermal Engineering*, 42, 178-187

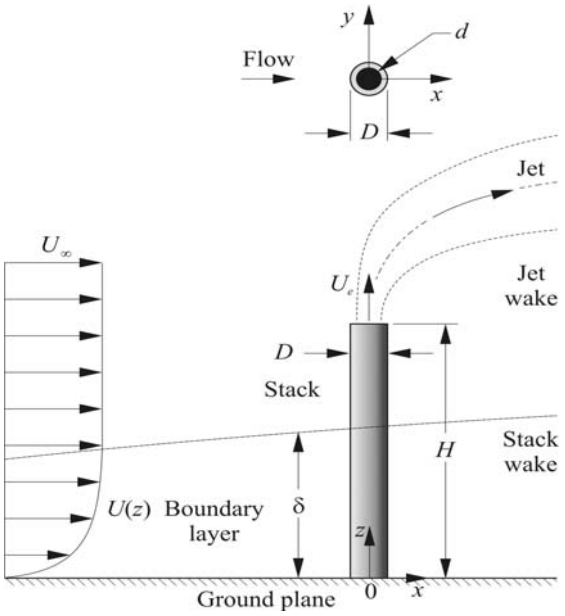

Figure 1: Schematic of a cylindrical stack mounted normal to a ground plane and partially immersed in a plane boundary layer.

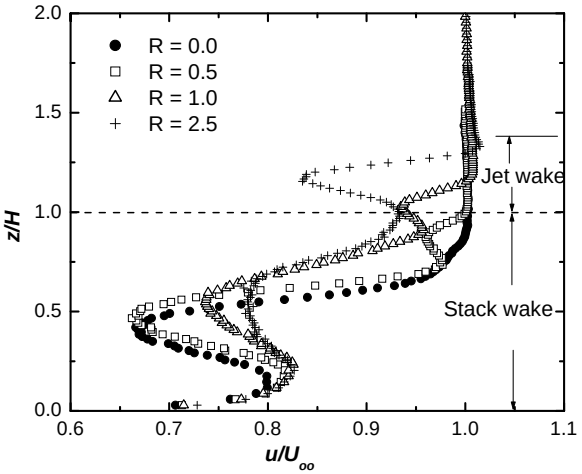

Figure 2: The time-averaged streamwise velocity profiles along the wake centreline ($y/D = 0$) at $x/D = 10$

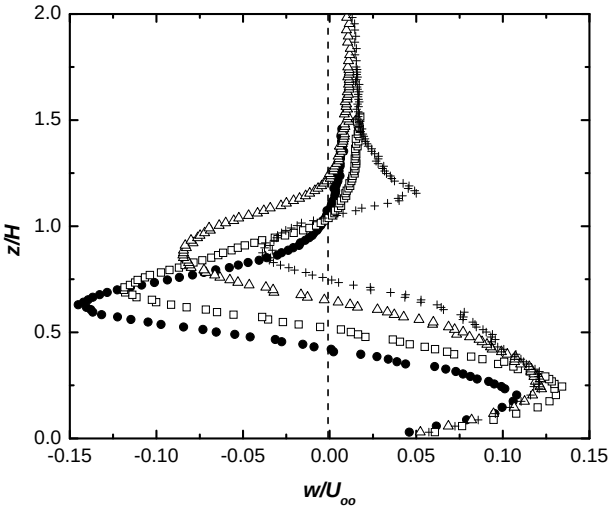

Figure 3: The time-averaged wall-normal velocity profiles along the wake centreline (y/D = 0) at x/D = 10 (symbols as defined in Figure 2)

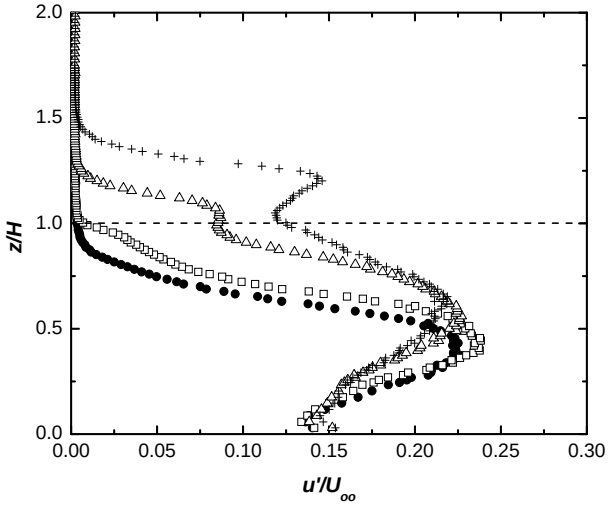

Figure 4: The streamwise turbulent intensity profiles along the wake centreline (y/D = 0) at x/D = 10 (symbols as defined in Figure 2)

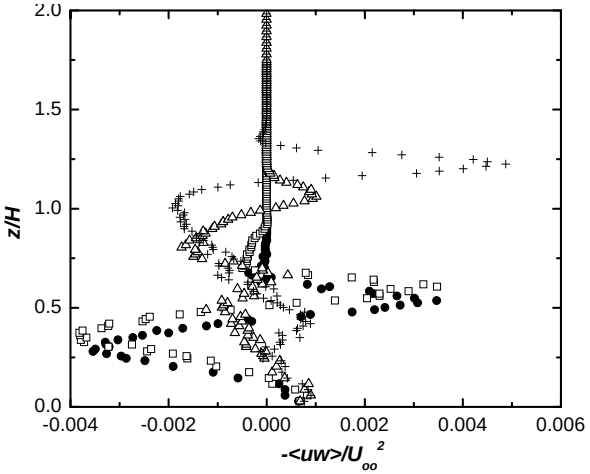

Figure 5: Reynolds shear stress profiles along the wake centreline (y/D = 0) at x/D = 10 (symbols as defined in Figure 2)

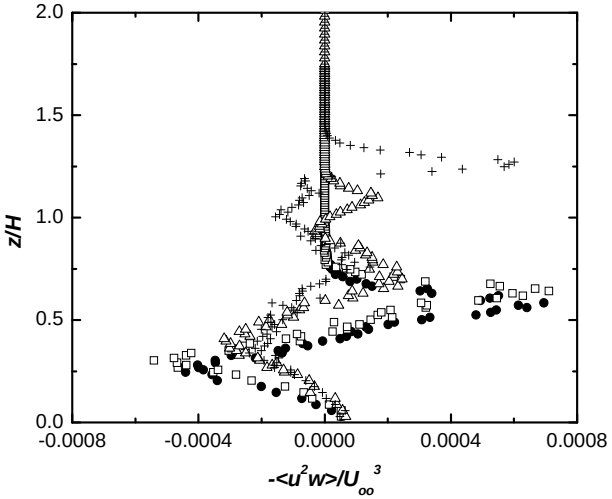

Figure 6: The $<u^2w>/U_{oo}^3$ profiles along the wake centreline (y/D = 0) at x/D = 10 (symbols as defined in Figure 2)

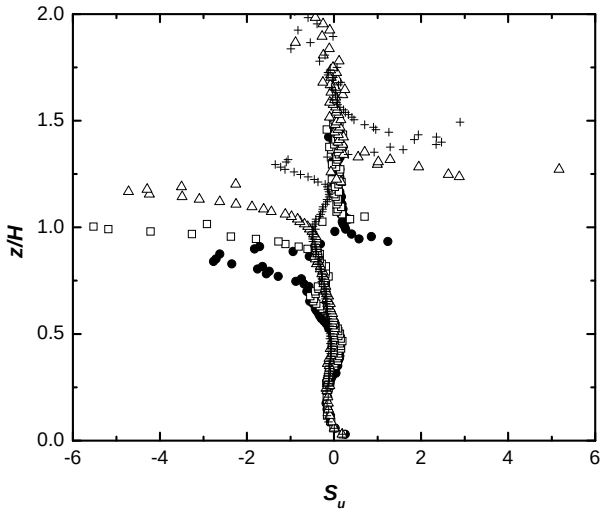

Figure 7: The streamwise skewness factor (S_u) profiles along the wake centreline (y/D = 0) at x/D = 10 (symbols as defined in Figure 2)

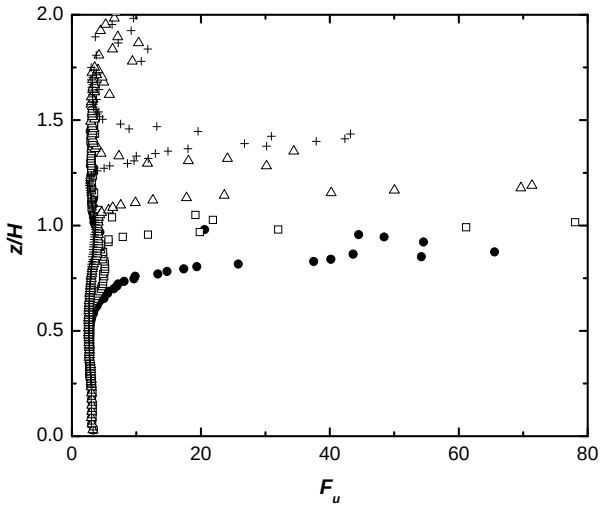

Figure 8: The streamwise flatness factor (F_u) profiles along the wake centreline (y/D = 0) at x/D = 10 (symbols as defined in Figure 2)